VISCOUS EFFECTS IN PARAMETRICALLY EXCITED WATER WAVES

José M. Vega

Dep. de Fundamentos Matemáticos
E.T.S.I. Aeronáuticos
Universidad Politécnica de Madrid.
Plaza Cardenal Cisneros, 3,
28040 Madrid, Spain.
Email: vega@fmetsia.upm.es

Abstract. The effect of viscosity is considered in the capillary-gravity waves that are parametrically excited by vertical vibrations in a horizontal fluid layer. Special attention is paid to the viscous mean flow generated by time averaged Reynolds stresses in the oscillatory boundary layers attached to the solid walls and the free surface. It is explained that this secondary mean flow affects the dynamics of the primary waves themselves. Several specific limiting cases of practical interest are considered to illustrate the consequences of this coupled evolution.

Key words: *Water waves, nearly inviscid flows, oscillatory flows, streaming flows.*

1. INTRODUCTION

As an homage to Amable Liñán in his 70th birthday, I describe below some results obtained in the last years by the applied mathematics group at the E.T.S.I. Aeronáuticos, in collaboration with the Physics department of the University of California at Berkeley. Since Amable himself is not participating in this review, the reader will not find here the mastery use of both mathematics and physical concepts that is always present in his work, but some trace can perhaps be found of various lessons that I learned as a graduate student of him.

The *small viscosity limit* is a singular limit in fluid mechanics and in the presence of (even weak) nonlinearity leads to fairly rich dynamics. This limit allows the application of *singular perturbation methods*, which both clarify subtle concepts and simplify the analysis, two advantages that become evident in the wise use of these methods by Amable Liñán.

Water waves have held fascination of fluid dynamicists and applied mathematicians since the XIX Century and are of interest in a variety of problems, ranging from the study of waves and currents in lakes and the ocean to the analysis of vibrating containers. The dynamics of strictly inviscid water waves were uncovered through the theoretical work by Stokes, Airy, Boussinesq, Rayleigh, and others. The simplest formulation includes dispersion and nonlinear effects, and leads to the Schrödinger and KdV equations, namely

$$A_t = \mathrm{i}\alpha A_{xx} + \mathrm{i}\beta|A|^2 A \quad \text{and} \quad h_t = \alpha h_{xxx} + \beta h h_x, \tag{1}$$

which are paradigms of soliton forming systems [1]. These equations apply in a moving reference frame that travels with the group velocity, which eliminates the effect of an additional convective term that is large compared to dispersion in the scaling that leads to both the Schrödinger and KdV equations.

Viscous effects play a non central role in the dynamics of *long* water waves encountered in lakes and the ocean. These exhibit a wavelength ℓ of the order of several meters and (since the kinematic viscosity is $\nu \simeq 1$ cm^2 s^{-1} for water) a viscous time, ℓ^2/ν, of the order of several days, which is too large compared to the usual observation times. The viscous time is much smaller, or the order of minutes, for the *short* waves generated in small vibrated containers, which are the object of this paper. Viscous effects are measured by the nondimensional parameter

$$\varepsilon = \frac{\nu}{\omega^* \ell^2} \ll 1, \tag{2}$$

where ω^* is the wave frequency, and produce a *linear damping* of the waves and a secondary *viscous mean flow*. The former comes in practice from several physically different sources and the latter affects the dynamics of the primary waves. Also, the presence of lateral walls where the waves are reflected and/or the nature of the forcing device, require to consider two *counterpropagating waves* at each point. Thus the effect of the group velocity cannot be eliminated and the relevant equations exhibit terms that are not of the same order. All these involve additional subtleties that will be discussed below.

In the sequel, I concentrate in extensions of the Schrödinger equation, which applies in deep containers, whose depth is at least comparable to wavelength.

2. LINEAR DAMPING

Linear damping adds a new term to the Schrödinger equation (1a), which becomes

$$A_t = \mathrm{i}\alpha A_{xx} - \delta A + \mathrm{i}\beta|A|^2 A. \tag{3}$$

All solutions to this equation converge to the basic state $A = 0$ for large time unless a forcing term is added either in the equation itself or in the boundary conditions. The damping ratio, $\delta > 0$, is small and may came from either of the following sources:

1. *Viscous dissipation* in both the oscillatory boundary layers attached to solid boundaries and the free surface, and the bulk, which are $O(\varepsilon^{1/2})$, $O(\varepsilon^{3/2})$, and $O(\varepsilon)$, respectively. For (small but) finite realistic values of ε, the $O(\varepsilon)$-correction is necessary to get a good agreement with the experiments, as pointed out in [2] to explain

earlier quite precise measurements in a cylindrical container [3]. The theory in [2] was extensively checked experimentally [4], with a completely satisfactory agreement.

2. *Surface contamination*, which is to be expected in water unless a lot of care is taken in the experimental set up, may increase the linear damping rate by a factor of 5 [3]. This effect is usually modeled through the effect of contaminant (insoluble) surfactants, which produce a tangential stress proportional to the tangential gradient of surfactant concentration [5, 6]. This effect can be so strong as to make the free surface almost inextensible, and completely changes the structure of the upper boundary layer, attached to the free surface. These (old) ideas have been applied to cylindrical containers [7], to obtain quantitative results that compare well with the experiments using tap water by Henderson and Miles [3]. The results are not so good as those for clean free surface due to uncertainties in the parameter values; note that the nature of surfactants is not known for tap water. Surface contamination has also an effect in the generation of mean flows, to be commented below.

3. *Contact line motion* promotes additional damping whose analysis requires a precise modeling of the dynamical contact angle, which remains laking nowadays. Contact line motion has other subtle effects in the structure of the viscous mean flow, but these are beyond the scope of this paper.

3. MEAN FLOWS

As in any physical problem involving oscillations, nonlinear terms promote (through the product of in phase oscillatory terms, as in, e.g., $2\sin^2 t = \cos 2t + 1$=oscillatory+steady) the appearance of steady (or slowly varying) terms that force a slowly varying *mean flow*. This can be slaved to the oscillatory solution, but can also exhibit its own dynamics and affect the weakly-nonlinear evolution of the primary oscillatory flow *provided that the linearized problem exhibits nearly marginal, nonoscillatory modes*. This is the case in water waves because these exhibit the so called *viscous, or hydrodynamical modes*, which are non-oscillatory and nearly marginal, involve a quite small free surface deflection, and exhibit nonzero vorticity everywhere. All these are in contrast with the *nearly-inviscid, or surface modes* that are directly responsible for water waves. These are also nearly marginal but they are oscillatory, involve a significant free surface deformation, and exhibit zero vorticity except in viscous boundary layers. Viscous modes of nearly inviscid waves had been known for decades [8]. Their role in promoting *the coupled evolution of the waves and the viscous mean flow*, however, has not been recognized until quite recently (see [9] for a recent review).

In fact, mean flows are produced in water waves by three different sources:

1. *The Stokes drift* [10] is a purely kinematical effect that results from nonlinearity in the ODEs that provide the trajectories of fluid elements, namely

$$\frac{d\boldsymbol{x}}{dt} = \boldsymbol{v}(\boldsymbol{x}, t), \tag{4}$$

where the vectors $\boldsymbol{x}$ and $\boldsymbol{v}$ stand for position and velocity, respectively. By the way, nonlinear terms in this equation can also yield in 3D chaotic behavior (sometimes called chaotic advection [11, 12]), which has nothing to do with (pre-) turbulent flows but is quite relevant in visualizations, transport of passive scalars, and mixing. The Stokes drift is slaved to the primary waves and thus has no dynamical consequences.

2. *The inviscid mean flow* is produced by nonlinear terms in the kinematical boundary condition at the free surface, and is present in classical strictly inviscid water wave descriptions [13]. The associated forcing term is a vertical forcing velocity at the unperturbed free surface, which is proportional to the square of the wave amplitude.

3. *The viscous mean flow* is produced by time averaged Reynolds stresses (which vanish in the bulk at leading order) in the oscillatory boundary layers. This flow was visualized already by Faraday in his seminal experiment [14] through the anomalous accumulation of sand near the bottom of a vertically vibrated container. A first analysis of the viscous mean flow was made by Rayleigh [15] in a pioneering analysis of the oscillatory boundary layer attached to a solid boundary. He also recognized that the same explanation applies to the accumulation of dust in sound tubes (or Kundt tubes), known as Kundt figures. He did not realize instead that averaged Reynolds stresses were high enough as to produce a nonzero tangential velocity at the edge of the boundary layer, which should force a viscous mean flow also in the bulk. This was analyzed much later by Schlichting [16], and extended to the boundary layer attached to a free surface by Longuet-Higgins [17]. This viscous mean flow (also known as steady streaming, or acoustic streaming [18]) has been studied in many contexts, but always as a byproduct of the primary waves. It took much more time to recognize that the secondary mean flow does affect the dynamics of the primary waves.

4. COUNTERPROPAGATING WAVES

Water waves are traveling waves that because of reflection symmetry can propagate to either side. Early studies of water waves were concerned with one sided waves. This restriction excludes many realistic configurations in which both waves are generated. Reflection at lateral walls and/or symmetric forcing (e.g., vertical vibrations of the container, which parametrically force the so called Faraday waves [19], the most studied example of water waves in finite containers) produce both counterpropagating waves. For the sake of clarity I add the parametric forcing effect of vertical vibrations, but this is unessential in the main points discussed below. Also, I will consider one-dimensional waves in a laterally unbounded fluid layer, and impose periodic boundary conditions in the horizontal direction. This 2D model is intended to mimic three-dimensional containers with an annular cross section.

Ignoring at the moment the mean flow, the nondimensional free surface elevation can be written as

$$h = A^+(x,t)\mathrm{e}^{\mathrm{i}(\omega t+kx)} + A^-(x,t)\mathrm{e}^{\mathrm{i}(\omega t-kx)} + \text{c.c.} + \ldots, \tag{5}$$

where $A^\pm$ are the small, slowly varying ($|A^\pm|_{xx} \ll |A^\pm_x| \ll |A^\pm|$, $|A^\pm_t| \ll |A^\pm| \ll 1$)

complex amplitudes of the envelopes of the two waves, which travel with phase velocities $\mp k/\omega$. The nondimensional frequency (a half of the forcing frequency because of parametric forcing [20]) and wavenumber satisfy the dispersion relation

$$\omega^2 = k[S + (1-S)k^2]\tanh kd + O(\sqrt{\varepsilon}), \tag{6}$$

where $S = \sigma/(\sigma + \rho g \ell^2)$ (with σ= surface tension, ρ=density, and g= gravitational acceleration), d is the nondimensional depth, and ε is as defined in (2). $A^{\pm}$ satisfy the amplitude equations cf.(3)

$$A^{\pm}_t = \pm v_g A^{\pm}_x + \mathrm{i}\alpha A^{\pm}_{xx} - \delta A^{\pm} + \mathrm{i}(\beta_1|A^{\pm}|^2 + \beta_2|A^{\mp}|^2)A^{\pm} + \mu\bar{A}^{\pm}, \tag{7}$$

where the coefficients $v_g \sim \alpha \sim \beta_1 \sim \beta_2 \sim 1$ and $\mu \sim \delta \ll 1$; these account for the group velocity, dispersion, nonlinear self and counter-interaction, parametric forcing, and damping, respectively. Thus the first term in the right hand side, which cannot be eliminated using moving axes, is large compared to the second term. The boundary conditions,

$$A^{\pm}(x+L,t) = \mathrm{e}^{\mp\mathrm{i}\tilde{\delta}}A^{\pm}(x,t), \tag{8}$$

result form spatial periodicity; the spatial detuning $\tilde{\delta} = 2kL \pmod{2\pi}$ accounts for the mismatch between the period of the waves and the imposed spatial period. Eqs.(7)-(8) are invariant under the actions $A^{\pm} \to A^{\pm}\mathrm{e}^{\pm\mathrm{i}c_1}$, $x \to x + c_2$ for all $c_1, c_2 \in \mathbb{R}$, $A^{+} \leftrightarrow A^{-}$, and $x \to -x$, which result from invariance of the original problem under the orthogonal group generated by reflection and x-translations. Those actions generate a larger group than the original one, the additional symmetries being an artifact of truncation.

The presence of the large term in the system (7) allows two possible scalings, depending on the comparative values of slow spatial scale $L \gg 1$ and the damping ratio δ.

- If $\delta \ll L^{-1}$ then the appropriate scaling is $L^{-1} \sim |\partial/\partial t| \sim |\partial/\partial x| \gg |A^{\pm}|^2$ and the equations (7) simplify to leading order to the homogeneous wave equations $A^{\pm}_t = \pm v_g A^{\pm}_x$, which give $A^{\pm} = A^{\pm}(\xi^{\pm}, \tau)$, where $\xi^{\pm} = (x \pm v_g t)/L$ are characteristic variables that involve two slow spatial and temporal scales, and $\tau \sim t/L^2$ is a still slower timescale in which forcing, damping, and nonlinearity are comparable. Applying a two-time scales method [21], it follows that the complex amplitudes evolve according to the following pair of nonlocal equations (after rescaling $\sqrt{\delta}$, $\sqrt{\mu}$, and $A^{\pm}$ with $1/L$ [22]),

$$A^{\pm}_{\tau} = \mathrm{i}\alpha A^{\pm}_{\xi^{\pm}\xi^{\pm}} - \delta A^{\pm} + \mathrm{i}(\beta_1|A^{\pm}|^2 + \beta_2\langle|A^{\mp}|^2\rangle)A^{\pm} + \mu\langle\bar{A}^{\mp}\rangle, \tag{9}$$

$$A^{\pm}(\xi^{\pm}+1,\tau) = \mathrm{e}^{\pm\mathrm{i}\tilde{\delta}}A^{\pm}(\xi^{\pm},\tau), \tag{10}$$

where $\langle\cdot\rangle$ stands for the spatial average. Note that coupling between both equations only occurs through the nonlocal term, whose appearance can be explained as follows. The waves are traveling in opposite directions with a velocity that is quite fast for the evolution in the slowest timescale, $\tau \sim 1$. Thus each wave only 'sees' the spatial mean value of the other wave. Nonlocal (Ginzburg-Landau-like) equations of this type had been already derived and analyzed for fully dissipative systems in various places ([23, 24] and references therein).

- If $\delta \sim L^{-1}$ then the group velocity term is balanced in first approximation by all terms, except dispersion, and after rescaling $1/t$, $1/x$, δ, μ, and $(A^{\pm})^2$ with $1/L$, eqs.(7)-(8) are rewritten as

$$A_t^{\pm} \mp v_g A_x^{\pm} = \mathrm{i}L^{-1}\alpha A_{xx}^{\pm} - \delta A^{\pm} + \mathrm{i}(\beta_1|A^{\pm}|^2 + \beta_2|A^{\mp}|^2)A^{\pm} + \mu\bar{A}^{\mp}, \tag{11}$$

$$A^{\pm}(x+1,t) = \mathrm{e}^{\pm \mathrm{i}\bar{\delta}} A^{\pm}(x,t), \tag{12}$$

  The analysis of this system requires some care because of the following facts:

  - Since $L \gg 1$, one is tempted to neglect dispersion (namely, set $L^{-1} = 0$ in (11)), to obtain a system of nonlinear hyperbolic equations that provide a coupled evolution of $A^{\pm}$, which in fact gives a good approximation of solutions of (11). But these can (and do [25]) develop discontinuities; near these, dispersion effects cannot be neglected. Also, smooth solutions of the hyperbolic equations can be *unstable* as (approximate) solutions of (11) *because of the presence of dispersion*. This is a subtle question (first solved for dissipative systems in [24, 26]) whose analysis requires to consider the stability of general solutions of the hyperbolic approximation against *dispersive scales*, with a wavelength of the order of $L^{-1/2}$, still large compared to the basic wavelength ($\sim L^{-1}$ with the scaling that leads to (11)) of the surface waves. This has been analyzed in [25], where it was seen that dispersive scales are in fact unstable in most part of the bifurcation diagrams, and lead to spatio-temporal chaos for sufficiently large forcing.
  - In the absence of diffusion, which is quite small in water waves, there is no an obvious mechanism to pack the spatial wave spectra around a given wavenumber and it may well happen that the solutions of (11)-(12) develop arbitrarily small scales. This is a central point that has been solved in related contexts (unforced, two dimensional waves) with some ingenuity. Namely, higher order dispersive terms, involving higher order spatial derivatives have been added that prevented the appearance of small scales [27]; small scales are also inhibited if the truncated (parabolic) linear dispersion relation of the primary waves that is implicit in the approximation (7) is replaced by the exact dispersion relation [28]. In the case of parametric forcing, this question has been solved 'numerically' after an order-of-magnitude analysis [25], noting that the wave spectra is effectively packed provided that not too many modes are considered, namely that the wave packet does not include the shortest basic length, $x \sim 1/L$ with the scaling that leads to (11). This shows that arbitrarily small scales are not produced if they are not present initially [25]. But an analytical proof of this property is lacking for parametric forcing and the problem remains open in more general situations.

5. COUPLED AMPLITUDE-MEAN FLOW EQUATIONS

The equations for counterpropagating waves considered above do not include the effect of the mean flow. This appears in a natural way when the simplified equations describing

the weakly nonlinear dynamics are derived from the original exact formulation (continuity and Navier-Stokes equations, with boundary conditions at the free boundary) via matched asymptotic expansions and two-time scales methods [29]. The mean flow adds an additional term (which has a counterpart in classical inviscid formulations [13]) in (7) that depends bilinearly on both $A^{\pm}$ and the horizontal component of the mean flow; see the last term in the right hand side of eq.(22) below. The viscous mean flow itself is given in the bulk (outside the oscillatory boundary layers) by some continuity and Navier-Stokes-like equations, with nonhomogeneous boundary conditions that include a tangential velocity (at solid boundaries) and a shear stress (at the free surface); these depend quadratically on the complex amplitudes $A^{\pm}$. The mean flow exhibits nonzero vorticity and in fact is responsible for vorticity transport from the edge of the boundary layers to the bulk. All these amount to a fairly complex system of *coupled amplitude-mean flow equations* [29] that is not amenable to reasonable analysis without further simplifications, like the ones made below for illustration in several, especially relevant particular cases

5.1. Drift instabilities of spatially constant waves

Drift instabilities, which lead to drifting patterns, appear when reflection symmetry is broken [30], and have been experimentally observed in spatially constant surface waves in vertically vibrated annular containers [31]. The origin of drift however is not clear in this case because spatially constant waves are reflection symmetric at leading order, see eq.(15) below. Thus, there is no a symmetry breaking mechanism in the waves themselves to trigger a drift instability. Let us see that the drift instability is due to a symmetry breaking of the associated viscous mean flow, which is thus essential to understand these drifting waves. In fact, ignoring the coupling of the surface waves to the mean flow leads to additional, related inconsistencies, which I discuss first. Assuming that $A^{\pm}$ are independent of x, the system (7) simplifies to the following system of (complex) ODEs,

$$dA^{\pm}/dt = -\delta A^{\pm} + \mathrm{i}(\beta_1|A^{\pm}|^2 + \beta_2|A^{\mp}|^2)A^{\pm} + \mu\bar{A}^{\pm}, \tag{13}$$

whose solutions are readily seen to converge for large time to a steady state of the form

$$A^{\pm} = Re^{-\mathrm{i}\omega\phi \mp \mathrm{i}k\psi}, \tag{14}$$

with R, ϕ, and ψ real constants. Substituting this into (5) gives the following expression for the free surface elevation

$$h = 4\cos\omega(t-\phi)\cos k(x-\psi), \tag{15}$$

which shows that the wave is a *standing wave*. Note that since ψ is constant, this wave exhibits no drift, which is consistent with the fact that it is reflection symmetric.

After appropriate nondimensionalization and scaling, the viscous mean flow produced

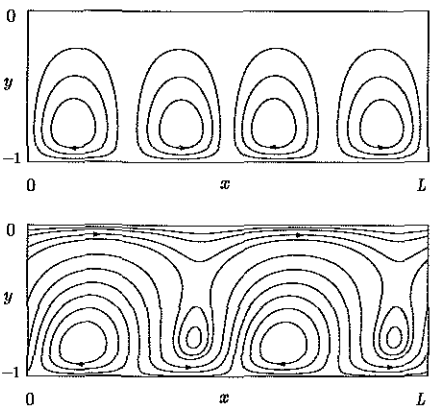

Figure 1. Streamlines of the stable steady state of (16)-(21) with $\psi = 0$, for $k = 2.37$, $L = 2\pi/k = 2.65$, and $Re = 35$ (upper plot) and 40 (lower plot). Courtesy of Elena Martín.

by this standing wave is given by the following well known set of equations [32]

$$u_x + v_y = 0, \tag{16}$$

$$\partial u/\partial t + v(u_y - v_x) = -q_x + Re^{-1}(u_{xx} + u_{yy}), \tag{17}$$

$$\partial v/\partial t - u(u_y - v_x) = -q_y + Re^{-1}(v_{xx} + v_{yy}), \tag{18}$$

$$u = -\sin 2k(x - \psi), \qquad v = 0 \quad \text{at } y = -1, \tag{19}$$

$$\partial u/\partial y = v = 0, \quad \text{at } y = 0, \tag{20}$$

$$u, \quad v \text{ and } q \quad \text{are } x\text{-periodic, of period } L = 2\pi/k, \tag{21}$$

where u and v are the horizontal and vertical mean flow velocity components, q is the associated stagnation pressure, ψ is the phase of the standing waves, which at the moment is assumed constant, and for consistency, I am imposing periodic boundary conditions, with the period of the waves; k is the nondimensional wavelength of the surface waves and $Re = \gamma R^2/\varepsilon$, with $\gamma \sim 1$, is the streaming flow Reynolds number. Since R and ε are independent of each other and small, Re varies in a wide range (typically, $0 < Re < 2000$).

For small Re, this system exhibits a unique, globally stable, reflection symmetric steady state that consists of an array of counterrotating eddies, like that plotted in fig.1 (upper plot). This solution was qualitatively described for large Re elsewhere [33] and has always been assumed (but never checked!) to be stable. It turns out that this is true only for not too large Re [34]. As Re increases, this steady state looses stability in a reflection-symmetry breaking bifurcation, and a new branch of non-symmetric steady states appears, see fig.1 (lower plot). The new solution exhibits a net horizontal velocity that is not compatible with the assumption that the waves are strictly standing (namely that the phase ψ is constant) because of advection by the streaming flow. This means that *the assumption that the surface waves are decoupled from the mean flow is inconsistent*, as

anticipated above.

Thus, the effect of the mean flow in the surface waves dynamics must be added, which is done replacing (13) by

$$dA^{\pm}/dt = -\delta A^{\pm} + \mathrm{i}(\beta_1|A^{\pm}|^2 + \beta_2|A^{\mp}|^2)A^{\pm} + \mu\bar{A}^{\pm} \mp \mathrm{i}L^{-1}\int_{-1}^{0}\int_{0}^{L} g(y)u\,dxdy\,A^{\pm}, \quad (22)$$

where

$$g(y) = 2k\cosh 2k(y+1)/\sinh 2k. \quad (23)$$

Note that $\int_{-1}^{0} g(y)\,dy = 1$, as required by invariance of the equations and boundary conditions at the upper boundary under the action $x \to x + ct$, $u \to u + c$, $\psi = \psi + ct$, which correspond to Galilean transformations.

Equations (16)-(21), and (22) can be further simplified trough the variable change

$$A^{\pm} = A_0^{\pm}\mathrm{e}^{\mp \mathrm{i}k\psi}, \quad (24)$$

where the spatial phase ψ is given by

$$d\psi/dt = L^{-1}\int_{-1}^{0}\int_{0}^{L} g(y)u\,dxdy. \quad (25)$$

Replacing this into (22), it follows that $A_0^{\pm}$ satisfy (13), which means that after an initial transient stage, $A_0^{\pm}$ converge to a steady state or, invoking (24) that the surface wave converges to a wave that is standing in a reference frame moving horizontally according to $x = \psi(t)$. The mean flow is again given by (16)-(21), with the spatial phase ψ no longer constant, but given by (25); these equations will be called below coupled phase shift-mean flow (CPSMF) equations. Note that eq.(25) gives precisely how the waves are advected by the mean flow, and is essential to understand drift instabilities. In particular, it shows that the drift velocity, $d\psi/dt$, vanishes if the mean flow is reflection symmetric as is the basic steady solution in fig.1a. Thus, *the origin of drift instabilities is* now clear: they are *associated with a symmetry breaking of the mean flow*, as anticipated above. Numerical integration of the CPSMF equations [34] shows that the mean flow stabilizes the reflection symmetric steady state; in fact, for $Re = 40$ the reflection-symmetric steady state of (16)-(21), (25) is still stable; it looses stability in a Hopf bifurcation at $Re = 270$ where a stable branch of *direction-reversing waves*, whose nodes oscillate back and forth is born; these solutions exhibit a periodic drift but no overall drift. Similar oscillatory (periodic, quasi-periodic, or chaotic) drifting solutions are obtained for other values of the parameters [34]. Steadily drifting solutions are also obtained, but only through secondary bifurcations. [34].

These results show that the origin of drift is connected with the viscous mean flow, which solves the main conceptual open problem mentioned above, but does not explain the experimental results in [31]. The main difference is that steadily drifted solutions were quite robust in the experiment [35] but only appear in secondary bifurcations in the CPSMF equations. This can be due to the fact that the experiment was done with tap water, which is strongly contaminated. As explained above, contamination completely

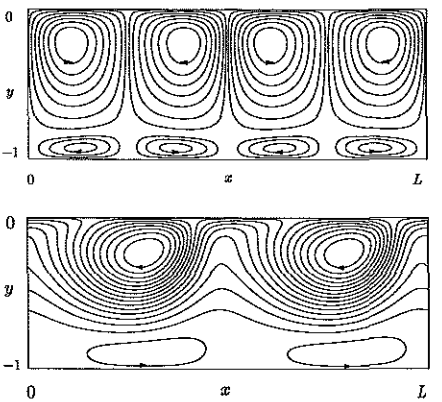

Figure 2. Streamlines of a reflection symmetric steady state for $Re = 60$ (upper plot) and a steadily drifting state, with a drift velocity $\psi' = -0.077$ for $Re = 200$ (lower plot), of the CPSMF equations (16)-(18), (25), (26)-(27), (29) ; the remaining parameters are $L = 2.65$, $k = 2.37$, and $\Gamma = 0.9$. The streamlines in the lower plot apply in moving axes, $x_{\text{mov}} = x_{\text{fixed}} - \psi' t$. Courtesy of Elena Martín.

changes (the boundary condition accounting for shear stress at the upper boundary and thus) the structure of the upper boundary layer, which in turn affects the boundary condition (20). This and (19) (which is also rescaled for convenience) are now

$$u = -(1-\Gamma)\sin 2k(x-\psi), \quad v = 0 \quad \text{at } y = -1, \tag{26}$$

$$u = -\Gamma \sin 2k(x-\psi) + u_0(t), \quad v = 0 \quad \text{at } y = 0, \tag{27}$$

where the net velocity u_0 is determined imposing the additional condition

$$\int_0^L u_y(x,0,t)\,dx = 0 \tag{28}$$

and $\Gamma > 0$ is a measure of contamination effects, which in the distinguished limit that leads to (27) are strong enough as to make the free surface almost inextensible. The additional condition (28) can be interpreted noting that the massless, inextensible free surface can balance a local shear stress from the flow, but not an overall stress, which would produce an infinite acceleration. The additional condition (28) does not apply when the 2D problem above is a model of a 3D annular container. In this case, the inner and outer walls of the container may have an effect if the surfactant monolayer exhibits a not too small surface shear viscosity, which can in fact prevent any overall motion of the monolayer. In this case, eq.(28) must be replaced by

$$u_0 = 0. \tag{29}$$

Numerical integration of the new CPSMF equations (16)-(18), (21), (25)-(27), and either (28) or (29) have shown [36] that for small Γ, the bifurcation diagrams are qualitatively similar to those of the non-contaminated case described above. This was not

necessarily so because the new boundary conditions (26)-(27) does not reduce to (19)-(20) as $\Gamma = 0$, which is due to the fact that the new boundary condition does not apply for too small Γ. An intermediate limit should be considered in which a mixed boundary condition (involving both the horizontal velocity and shear stress) applies; but this limit yields results that are qualitatively similar to those obtained in the clean case considered above. For larger values of Γ, the primary bifurcation from the basic steady state is a *parity breaking* bifurcation [30], which yields a new branch of *steadily drifting waves* like that plotted in fig.2 (lower plot), where the basic stable reflection symmetric state for $Re = 60$ is also plotted for comparison. For the parameter values in fig.2, the parity breaking bifurcation occurs at $Re_c = 109.8$ and the branch of steadily drifting solutions remains stable in the range $Re_c < Re < 433.2$. These solutions are $(L/2)$-periodic in the horizontal direction (lower plot in fig.2). At $Re = 433.2$ there is a spatial period doubling bifurcation that yields a new branch of L-periodic steadily drifting solutions, which remains stable for larger values of Re. These steadily drifting solutions remain stable when the horizontal length L is doubled and thus are quite robust, which is in complete accordance with experiments.

5.2. Standing waves near threshold

Near threshold, parametric forcing favors an equal superposition of both counterpropagating waves (namely, $|A^+| \simeq |A^-|$), which as in last section produces a *standing wave*. But if the aspect ratio is sufficiently large, spatial modulation cannot be ignored, and the relevant equation for the standing wave amplitude, $A \simeq A^{\pm}$, is a Ginzburg-Landau equation,

$$\varepsilon A_t = \beta_1 A_{xx} + \tilde{\mu} A - \varepsilon^2 \beta_5 |A|^2 A, \tag{30}$$

where all coefficients are real, the bifurcation parameter $\tilde{\mu}$ is a scaled measure of departure from threshold, and the small parameter ε is as defined in (2). This equation can be derived from (7) provided that some higher order terms accounting for nonlinear damping, nonlinear forcing, and a viscous correction to the group velocity are added. Note that eq.(30) is fully dissipative, which could be surprising at first sight because nonlinear terms are strictly conservative in the original counterpropagating waves equations; diffusion, in particular, comes from a balance between transport at the group velocity, linear damping, and linear forcing. Note that although $A \simeq A^{\pm}$, eq.(30) is not obtained setting $A^{\pm} = A$ in (7), which cannot be done unless $A^{\pm}$ are spatially constant. The derivation of (30) requires to consider two higher order corrections to the approximate relation $A^{\pm} \simeq A$ [37].

Equation (30) can also be derived without the assumption of small viscous effects [38], to check the asymptotic expression of β_5 for small ε, whose repeated derivation in the literature has been controversial [39]. To our surprise [38], none of the asymptotic expressions in the literature matched with the exact value of β_5. Moreover, β_5 shows a surprising dependence on wavenumber; namely, a $O(\varepsilon^2)$-shift on the wavenumber produced a $O(1)$-correction on β_5. This was not due to any mistake in the viscous calculation of β_5 performed in [38], which perfectly matched with former independent calculations by Chen and Viñals [40] (who did not notice this surprising dependence on wavenumber).

This high sensitivity to wavenumber shift cannot be understood in the context of the Ginzburg-Landau equation (30): a $O(\varepsilon^2)$-shift on wavenumber is accounted for replacing A by $Ae^{\varepsilon^2\kappa x}$, which produces a new term proportional to $\mathrm{i}\varepsilon^2 A_x$ and a $O(\varepsilon^4)$-correction in the bifurcation parameter $\tilde{\mu}$, but has no effect on β_5. The effect can neither be understood in the context of the more general quintic equation first guessed (not derived) by Milner [41],

$$\varepsilon A_t = \beta_1 A_{xx} + \tilde{\mu} A - \varepsilon^2 \beta_5 |A|^2 A - \beta_2 |A|^4 A, \tag{31}$$

which has been always taken from granted but has never been derived. This confused situation could only be clarified by trying to derive Milner equation from the original counterpropagating equations (corrected with higher order terms as indicated above). This has been done in [37], where it was shown that, in addition, the viscous mean flow (also ignored by Milner) produces a new term that was comparable to the remaining ones in Milner equation. It follows that the correct description of the standing waves is given by

$$\varepsilon A_t = \beta_1 A_{xx} + \tilde{\mu} A - \varepsilon^2 \beta_5 |A|^2 A - \beta_2 |A|^4 A + \mathrm{i}\beta_4 |A|^2 A_x + \mathrm{i}\beta_3 (|A|^2)_x A + \mathrm{i}\beta_6 h_x A, \tag{32}$$

where h is the (slowly varying) free surface elevation associated with the viscous mean flow and is given by the following equation

$$\varepsilon h_t = \beta_7 h_{xx} + \beta_8 (|A|^2)_{xx}, \tag{33}$$

which is a balance between inertia, the restoring action of gravity, and the forcing effect of the surface waves. Note that now, because of the new term proportional to $\mathrm{i}|A|^2 A_x$, a $O(\varepsilon^2)$ wavenumber shift does produce a $O(1)$ correction on β_5. The various coefficients in this equation have been derived in closed form in [37] and checked with their exact counterparts calculated numerically in the viscous limit [38]. In particular, the asymptotic expression for the cubic coefficient shows the above mentioned sensitivity on wavenumber shift, and does match with its exact value for small ε, see fig.3. Note that the agreement is quite good, except in a vicinity of $\Gamma = 1/3$, where the asymptotic value of β_5 diverges due to a well known 2:1 resonance (the inviscid dispersion relation (6) is such that $\omega(2k) = 2\omega(k)$).

Note that all terms in (32)-(33) can be made of the same order under appropriate scaling. Thus, the new terms in (32) do not account for higher order effects, but do have a $O(1)$ effect in the dynamics when the ratio between the parameters $\varepsilon \ll 1$, $L \gg 1$, and $\tilde{\mu} \ll 1$ is appropriate. In fact, the new terms have two qualitative effects, which are expected to change the dynamics dramatically. Namely:

1. They prevent the existence of the Lyapunov function exhibited by Milner equation.

2. They break a spurious reflection symmetry of Milner equation, which is invariant under the actions $x \to -x$ and $A \to \bar{A}$ separately, while (32) is only invariant under the joint action $(x, A) \to (-x, \bar{A})$.

Some preliminary calculations by Dr. María Higuera have shown that eqs.(32)-(33) do in fact exhibit oscillatory instabilities, which cannot be present in Milner equation.

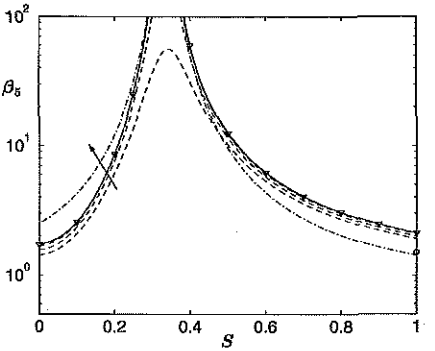

Figure 3. The coefficient β_5 appearing in eqs.(30)-(32 in terms of the gravity-capillary balance parameter S, defined just after eq.(6). (——) Asymptotic value as $\varepsilon \to 0$; (- - -) as calculated in [38] for $\varepsilon = 1.25 \cdot 10^{-2}$, $5 \cdot 10^{-3}$, and $5 \cdot 10^{-4}$ (the arrows indicate decreasing values of ε); (— · — · —) as calculated in [42] for $\varepsilon = 0$; (∇) as calculated in [40] for $\varepsilon = 5 \cdot 10^{-4}$; (o) as calculated (for $\varepsilon = 0$) in [39], where only the capillary limit was considered . Courtesy of Francisco Mancebo.

5.3. Modulated counterpropagating waves at large aspect ratio

The analysis in last section requires that the forcing amplitude be conveniently close to its threshold value. Outside this vicinity of threshold, both counterpropagating waves must be considered separately. In this case, the general coupled amplitude-mean flow equations can only be simplified under additional assumptions concerning detuning [29, 43] and the ratio of the container depth to wavelength [29, 44]. If the latter is large, the mean flow is almost parallel and both inertia and convective terms can be neglected in momentum equations, allowing a numerically cheap integration of the resulting simplified equations [44], which however exhibit the subtleties mentioned in §4 in connection with eq.(11). It follows that the main overall effects of the mean flow are (i) to inhibit dispersive scales and the associated spatio-temporal chaotic behavior, and (ii) to promote oscillatory instabilities. Reflection symmetry is typically broken in gravity waves (which therefore exhibit drifting patterns), but is inhibited for capillary waves. Note that the origin of drift is now associated with wave modulation, and thus quite different from that described in §5.1.

5.4. Small aspect ratio containers

A complete theory for parametrically excited water waves in small aspect ratio containers (with a width comparable to wavelength) has been developed [45, 46], extending previous related results on one-mode capillary waves in the liquid bridge geometry [47]. The surface waves are described by a finite number of modes. The coupled amplitude-mean flow equations for that case have shown that the surface waves are affected by the viscous mean flow whenever more than one surface mode is present, as in the seminal ex-

periments by Ciliberto and Gollub [48] (two pairs of non-axisymmetric modes in circular containers) and Simonelli and Gollub [49] (two modes in almost square containers). Some predictions (e.g., existence of relaxation oscillations and canard behavior [50, 51]) have been also made [52] for a case that is potentially interesting and has not been checked experimentally, namely the case a single pair of nonaxisymmetric modes in an almost circular container.

5.5. Two dimensional waves at large aspect ratio

Two dimensional waves in large aspect ratio (three dimensional) containers show a great variety of patterns [53]. The first bifurcation from the flat state yields standing wave rolls, squares, hexagons, or quasipatterns, depending on the various non-dimensional parameters, and has been completely explained by Viñals and collaborators [42, 40], whose theory has been experimentally checked with great precision [54]. This primary bifurcation is not affected by the viscous mean flow, which is consistent with the fact that Viñals quasipotential theory ignores the mean flow. This theory has not been successful in explaining the remaining instabilities [55] beyond the first one. The mean flow can be added to Viñals theory fairly straightforwardly, but gives coupled amplitude-mean flow equations whose numerical integration is too expensive [56] because they involve three-dimensional Navier-Stokes-like equations. Thus, we have introduced a cascade of simpler equations [56] that are more tractable. The last step is a toy model, in the spirit of the Swift-Hohenberg equations [57], which have shown that the mean flow does affect the surface wave dynamics, promoting a new oscillatory instability and modifying the various instability boundaries that already existed in Viñals theory. But this is only a first step in the correct analysis of two dimensional waves, which remains essentially undone.

6. CONCLUDING REMARKS

The effect of small viscosity in water waves has been considered, focusing in the generation of a *viscous mean flow*, which is a second order effect, namely its strength depends quadratically on the wave amplitude. Thus, in the shorter timescale associated with wave oscillation, the mean flow only produces a small drift of material elements. In the slower timescale associated with wave modulation instead, the mean flow produces an effect that is of the same order as that of the cubic nonlinear terms that saturate the dynamics, and thus it affects the dynamics of the primary waves in an essential way. This has not been noticed in previous analyses of surface waves, perhaps because (in contrast with the analysis reviewed above) equations had not been derived from first principles in a consistent way, except in the strictly inviscid case. Viscous effects, which are responsible for the appearance of the mean flow had been added *a posteriori* to the classical Hamiltonian formulations, through some *ad hoc* terms accounting for linear (and nonlinear) damping.

Unfortunately, without further simplifying assumptions, the mean flow obeys Navier-Stokes-like equations, which makes it difficult to extract precise predictions from the general coupled amplitude-mean flow equations. To make things worse, the amplitude equations exhibit their own subtleties in large aspect ratio systems (the natural candidates to simplify the mean flow equations) due to the interplay between advection at the group

velocity and dispersion. Thus, *simplicity* is not easily attained in the analysis of nearly-inviscid water waves in small containers. *Rigor* (which does not mean to only accept results stated as theorems) is essential to construct a theory that puts some order in the (largely unexplained) fascinating complexity observed in experiments, which are the final judges of scientific *relevance*.

Acknowledgements. The work reviewed in this paper has been made in collaboration with María Higuera, Edgar Knobloch, Victoria Lapuerta, Paco Mancebo, Carlos Martel, Elena Martín, José A. Nicolás, Sten Rüdiger, and Jorge Viñals. Continuous funding from NASA (Grants NAG3-2152 and NNC04GA47G) and the Spanish Ministry of Education (Grants PB97-0556 and BFM2001-2363) is also acknowledged.

REFERENCES

[1] A.C. Newell. *Solitons in Mathematics and Physics.* Society for Industrial and Applied Mathematics, 1985.

[2] C. Martel, J.A. Nicolás, and J.M. Vega. Surface-wave damping in a brimful circular cylinder. *J. Fluid Mech.* **360**, 213–228 (1998). See also Corrigendum **373**, 379 (1998).

[3] D.M. Henderson and J.W. Miles. Surface-wave damping in a circular cylinder with a fixed contact line. *J. Fluid Mech.* **275**, 285–299 (1994).

[4] D. Howell, T. Heath, C. McKenna, W. Hwang, and M.F. Schatz. Measurements of surface-wave damping in a container. *Phys. Fluids* **12**, 320–326 (2000).

[5] V.G. Levich. *Physicochemical Hydrodynamics.* Prentice-Hall, 1962.

[6] J.W. Miles. Surface wave damping in closed basins. *Proc. Roy. Soc. Lond.* **A297**, 459–473 (1967).

[7] J.A. Nicolás and J.M. Vega. A note on the effect of surface contamination in water wave damping. *J. Fluid Mech.* **410**, 367–373 (2000).

[8] H. Lamb. *Hydrodynamics.* Cambridge University Press, 1932.

[9] E. Knobloch and J.M. Vega. Nearly-inviscid Faraday waves. In P. Newton, P. Holmes, and A. Weinstein, editors, *Geometry, Mechanics and Dynamics: Volume in Honor of the 60th Birthday of J.E. Marsden*, pages 181–222. Springer-Verlag, 2002.

[10] G.G. Stokes. On the theory of oscillatory waves. *Trans. Camb. Phil. Soc.* **8**, 441–455 (1847).

[11] H. Aref. Stirring by chaotic advection. *J. Fluid Mech.* **212**, 337–356 (1984).

[12] M. Umeki. Lagrangian motion of fluid particles induced by three-dimensional standing surface waves. *Phys. Fluids* **A4**, 1968–1978 (1992).

[13] A. Davey and S. Stewartson. On three-dimensional packets of surface waves. *Proc. R. Soc. London* **A338**, 101–110 (1974).

[14] M. Faraday. On the forms and states assumed by fluids in contact with vibrating elastic surfaces. *Phil. Trans. Roy. Soc. London* **121**, 319–340 (1831).

[15] J.W.S. Lord Rayleigh. The circulation of air observed in Kundt's tubes, and on some allied acoustical problems . *Phil. Trans. Roy. Soc. London* **175**, 1–21 (1883).

[16] H. Schlichting. Berechnung ebener periodischer Grenzschichtströmungen. *Phys. Z.* **33** 327 –335 1932.

[17] M.S. Longuet-Higgins. Mass transport in water waves. *Phil. Trans. Roy. Soc.* **A245**, 535–581 (1953).

[18] N. Riley. Steady streaming. *Annu. Rev. Fluid Mech.* **33**, 43–65 (2001).

[19] J. Miles and D. Henderson. Parametrically forced surface waves. *Annu. Rev. Fluid Mech.* **22**, 143–165 (1990).

[20] S. Fauve. Parametric instabilities. In G. Martínez Mekler and T.H. Seligman, editors, *Dynamics of Nonlinear and Disordered Systems*, pages 67–115. World Scientific, 1995.

[21] S.C. Chekwendu and J. Kevorkian. A perturbation method for hyperbolic equations with small nonlinearities. *SIAM J. Appl. Math.* **22**, 235–248 (1972).

[22] C. Martel, E. Knobloch, and J.M. Vega. Dynamics of counterpropagating waves in parametrically forced systems. *Physica D* **137**, 94–123 (2000).

[23] J.M. Vega. On the amplitude equations arising at the onset of the oscillatory instability in pattern formation. *SIAM J. Math. Anal.* **24**, 603–617 (1993).

[24] C. Martel and J.M. Vega. Finite size effects near the onset of the oscillatory instability. *Nonlinearity* **9**, 1129–1171 (1996).

[25] C. Martel, J.M. Vega, and E. Knobloch. Dynamics of counterpropagating waves in parametrically driven systems: dispersion vs. advection. *Physica D* **174**, 198–217 (2003).

[26] C. Martel and J.M. Vega. Dynamics of a hyperbolic system that applies at the onset of the oscillatory instability. *Nonlinearity* **11**, 105–142 (1998).

[27] K. Trulsen and K.B. Dysthe. A modified nonlinear Schrödinger equation for broader bandwidth gravity waves on deep water. *Wave Motion* **24**, 281–289 (1996).

[28] K. Trulsen, I. Kliakhandler, K.B Dysthe, and M.G. Velarde. On weakly nonlinear modulation of waves in deep water. *Phys. Fluids* **12**, 2432–2437 (2000).

[29] J.M. Vega, E. Knobloch, and C. Martel. Nearly inviscid Faraday waves in annular containers of moderately large aspect ratio. *Physica D* **154**, 313–336 (2001).

[30] J.D. Crawford and E. Knobloch. Symmetry and symmetry-breaking bifurcations in fluid mechanics. *Annu. Rev. Fluid Mech.* **23**, 341–387 (1991).

[31] S. Douady, S. Fauve, and O. Thual. Oscillatory phase modulation of parametrically forced surface waves. *Europhys. Lett.* **10**, 309–315 (1989).

[32] M. Iskandarani and P.L.F. Liu. Mass transport in three-dimensional water waves. *J. Fluid Mech.* **231**, 417–437 (1991).

[33] A.K. Liu and S.H. Davis. Viscous attenuation of mean drift in water waves. *J. Fluid Mech.* **81**, 63–84 (1977).

[34] E. Martín, C. Martel, and J.M. Vega. Drift instability of standing Faraday waves in an annular container. *J. Fluid Mech.* **467**, 57–79 (2002).

[35] S. Fauve. Private communication. 2004.

[36] E. Martín and J.M. Vega. The effect of surface contamination on the drift instability of standing Faraday waves. *J. Fluid Mech., submitted*, 2004.

[37] F.J. Mancebo and J.M. Vega. Standing wave description of nearly inviscid, parametrically driven waves in extended systems. *Physica D, submitted*, 2004.

[38] F.J. Mancebo and J.M. Vega. Viscous Faraday waves in 2D large aspect ratio containers. *J. Fluid Mech., submitted*, 2004.

[39] P.L. Hansen and P. Alstrom. Perturbation theory of parametrically driven capillary waves at low viscosity. *J. Fluid Mech.* **351**, 301–344 (1997).

[40] P. Chen and J. Viñals. Amplitude equation and pattern selection in Faraday waves. *Phys. Rev. E* **60**, 559–570 (1999).

[41] S.T. Milner. Square patterns and secondary instabilities in driven capillary waves. *J. Fluid Mech.* **225**, 81–100 (1991).

[42] W. Zhang and J. Viñals. Pattern formation in weakly damped parametric surface waves. *J. Fluid Mech.* **336**, 301–330 (1997).

[43] J.M. Vega and E. Knobloch. Dynamics of counterpropagating waves in parametrically forced, large aspect ratio, nearly conservative systems with nonzero detuning. *Fluid Dyn. Research* **33**, 113–140 (2003).

[44] V. Lapuerta, C. Martel, and J.M. Vega. Weakly-dissipative Faraday waves in 2D large aspect ratio annuli. *Physica D* **173**, 178–203 (2002).

[45] M.J. Higuera, J.M. Vega, and E. Knobloch. Interaction of nearly-inviscid, multimode Faraday waves and mean flows. In L.L. Bonilla, G. Platero, D. Reguera, and J.M. Rubi, editors, *Coherent Structures in Complex Systems*, pages 328–337. Springer-Verlag, 2001.

[46] M.J. Higuera, J.M. Vega, and E. Knobloch. Coupled amplitude-mean flow equations for nearly-inviscid Faraday waves in moderate aspect ratio containers. *J. Nonlinear Sci.* **12**, 505–551 (2002).

[47] J.A. Nicolás and J.M. Vega. Weakly nonlinear oscillations of axisymmetric liquid bridges. *J. Fluid Mech.* **328**, 95–128 (1996).

[48] S. Ciliberto and J.P. Gollub. Chaotic mode competition in parametrically forced surface waves. *J. Fluid Mech.* **158**, 381–398 (1985).

[49] F. Simonelli and J.P. Gollub. Surface wave mode interactions: effects of symmetry and degeneracy. *J. Fluid Mech.* **199**, 471–494 (1989).

[50] M. Brons and K. Bar-Eli. Canard explosions and excitation in a model of the Belousov-Shabotinsky reaction. *J. Chem. Phys.* **95**, 8706–8713 (1991).

[51] J. Guckenheimer, K. Hoffman, and W. Weckesser. Numerical computation of canards. *Int. J. Bif. Chaos* **10**, 2669–2687 (2000).

[52] M.J. Higuera, E. Knobloch, and J.M. Vega. Dynamics of nearly-inviscid Faraday waves in almost circular containers. *Physica D, submitted*, 2004.

[53] A. Kudrolli and J.P. Gollub. Patterns and spatio-temporal chaos in parametrically forced surface waves: A systematic survey at large aspect ratio. *Physica D* **97**, 133–154 (1997).

[54] M.-T. Westra, D.J. Binks, and W. van de Water. Patterns of Faraday waves. *J. Fluid Mech.* **496**, 1–32 (2003).

[55] W. Zhang and J. Viñals. Numerical study of pattern formation in weakly damped parametric surface waves. *Physica D* **116**, 225–243 (1998).

[56] J.M. Vega, J. Viñals, and S. Rüdiger. Interaction of weakly damped Faraday waves and the associated mean flow in deep 3D containers of large aspect ratio. *Phys. Rev. E, submitted*, 2004.

[57] M.C. Cross and P.C. Hohenberg. Pattern formation outside of equilibrium. *Rev. Modern Phys.* **65**, 851–1112 (1993).